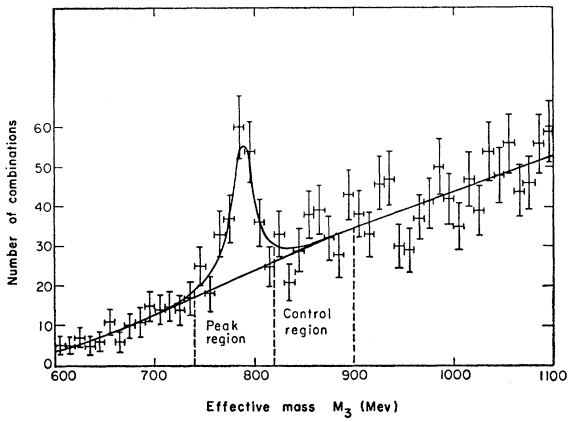

FIG. 3. Number of $\pi^+\pi^-\pi^0$ triplets vs effective mass (M_3) of the triplets for the reaction $\bar{p}+p \rightarrow 2\pi^+ + 2\pi^- + \pi^0$. The smooth curve drawn through the background has superposed upon it the experimental resolution function ($\Gamma_{\text{resol}}/2 = 12$ Mev). The area under the resolution function is equal to the number of events above the background curve.

the Dalitz plot. This is certainly inconsistent with the data. We must conclude that the ω is a vector meson, $J=1^-$.

Figure 3 shows a portion of the effective-mass distribution. A smooth curve has been drawn through the background and a curve (centered at $M_3=787$ Mev) that represents our experimental resolution function ($\Gamma_{\text{resol.}}/2=12$ Mev) has been superposed upon it. The area under the resolution function is equal to the number of events that lie above the background curve in the vicinity of the peak. The data reasonably fit the resolution function. We conclude that the true half-width $\Gamma/2$ is consistent with zero, and is less than 12 Mev.

Finally, we have studied angular distributions and correlations in ω meson breakup for the 270 triplets in the peak region. Within statistics, the ω meson is produced isotropically. We define the production normal $\mathbf{n}_1$ as $\mathbf{p}(\text{beam})\times\mathbf{p}(\omega)$. The breakup normal $\mathbf{n}_3$ (in the ω rest frame) is the direction normal to its breakup plane. We find that $\mathbf{n}_3$ is isotropic with respect to $\mathbf{n}_1$, to $\mathbf{p}(\text{beam})$, and to $\mathbf{p}(\omega)$. It is not correlated to the direction of breakup of the opposing dipion made in reaction (1).

We wish to point out that although our statistics are sufficiently good to allow a Dalitz-type analysis to be made, they are not such for the analysis of the angular distribution and correlations; a separate study must be made.

We again acknowledge the help that we received from those we mentioned in our earlier Letter. We regret that reference 9 of that Letter was garbled.[4] We also neglected to refer to the theoretical predictions of the ω by Fujii[5] and Breit.[6] We are indebted to Professor J. Sakurai for pointing this out to us.

[4] The last part of reference 9 should have read: For previous evidence see: I. Derado, Nuovo cimento **15**, 853 (1960); E. Pickup, F. Ayer, and E. O. Salant, Phys. Rev. Letters **5**, 161 (1960); J. G. Rushbrooke and D. Radojčić, *ibid.* **5**, 567 (1960); J. Anderson, V. Bang, P. Burke, D. Carmony, and N. Schmitz, *ibid.* **6**, 365 (1961); A. R. Erwin, R. March, W. D. Walker, and E. West, *ibid.* **6**, 628 (1961); D. Stonehill, C. Baltay, H. Courant, W. Fickinger, E. C. Fowler, H. Kraybill, J. Sandweiss, J. Sanford, and H. Taft, *ibid.* **6**, 624 (1961).

[5] Y. Fujii, Progr. Theoret. Phys. (Kyoto) **21**, 232 (1959).

[6] G. Breit, Proc. Natl. Acad. Sci. U. S. **46**, 746 (1960); Phys. Rev. **120**, 287 (1960).

PHYSICAL REVIEW VOLUME 125, NUMBER 2 JANUARY 15, 1962

$\pi^{\pm}-p$ Total Cross Sections in the Range 450 to 1650 Mev

THOMAS J. DEVLIN, BURTON J. MOYER, AND VICTOR PEREZ-MENDEZ
Lawrence Radiation Laboratory, University of California, Berkeley, California

(Received August 17, 1961)

The total cross sections for positive and negative pions on hydrogen were measured at frequent intervals in the energy range from 450 to 1650 Mev. Six scintillation counters measured the transmission of pions at various solid angles, and the results were extrapolated to zero solid angle. The two peaks previously discovered in the π^--p cross section were observed to be centered at 600 ± 15 Mev and 900 ± 15 Mev. A broad maximum was observed in the π^+-p cross section at approximately 1350 Mev. A "shoulder" at approximately 800 Mev, in a region where the π^+-p cross section is rapidly rising, supports speculation that there is a resonant state at this energy. Except for a small, unresolved difference in absolute values in the π^+-p case, these data agree with those obtained by Brisson *et al.* at Saclay.

I. INTRODUCTION

PRIOR to 1955, little work was done in the investigation of pion-proton scattering above 300 Mev.[1] Since that time, experiments have indicated that there is important structure in the graph of total cross section vs energy from 300 Mev to 2 Bev. Investigations at the Brookhaven Cosmotron[2] indicated the presence of broad maxima in the $\pi^- - p$ cross section near 900 Mev, and in the $\pi^+ - p$ cross section near 1.4 Bev. A group

[1] H. Bethe and F. de Hoffmann, *Mesons and Fields*, (Row, Peterson and Company, Evanston, Illinois, 1955), Vol. 2. This reference contains a summary of work done before 1955.

[2] R. Cool, O. Piccioni, and D. Clark, Phys. Rev. **103**, 1082 (1956).

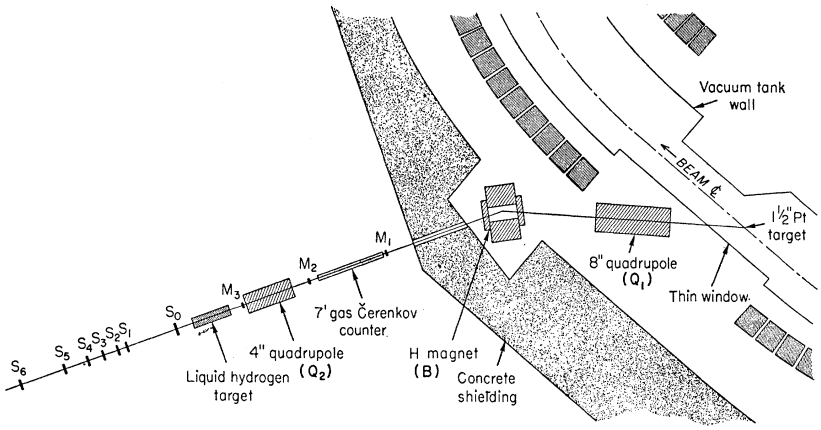

FIG. 1. Plan view of experimental arrangements.

from the Massachusetts Institute of Technology working at the Berkeley Bevatron resolved the broad maximum in the π^--p cross section into two peaks,[3] although the energies at which they observed these peaks were somewhat higher than those expected from the corresponding peaks in the pion photoproduction cross section.[4] In the π^--p cross section measurements of Brisson *et al.* at Saclay,[5] and in the measurements described here, this discrepancy does not exist. The results of the present experiment have received preliminary publication in part[6,7]; this article describes the work and analyzes the results more completely.

The following criteria were used in designing the experiment: (1) accurate determination of kinetic energy (1 to 2%); (2) good statistical accuracy (2%); (3) measurement of π^+-p and π^--p cross sections under the same experimental conditions for use in dispersion relations, and for determination of cross section for the isotopic spin ($T=\frac{1}{2}$) state; (4) accurate determination of beam contamination by particles other than pions, the effect of Coulomb scattering, and other spurious effects.

No formal theory yet exists allowing a calculation of the expected pion-proton cross section in this energy range; however, the results of experiments can yield qualitative information about the nature of the interaction.[4] A primary aim was the provision of some information about the quantum numbers involved if the peaks are due, in fact, to resonant states.

[3] H. C. Burrowes, D. O. Caldwell, D. H. Frisch, D. A. Hill, D. M. Ritson, R. A. Schluter, and M. A. Wahlig, Phys. Rev. Letters **2**, 119 (1959).

[4] Ronald F. Peierls, Phys. Rev. **118**, 325 (1960).

[5] J. C. Brisson, J. Detoeuf, P. Falk-Vairant, L. Van Rossum, G. Valladas, and L. C. L. Yuan; Phys. Rev. Letters **3**, 561 (1959); Nuovo cimento **19**, 210 (1961). Also see the author's report in *Proceedings of the 1960 Annual International Conference on High-Energy Physics at Rochester* (Interscience Publishers, Inc., New York, 1960), p. 38.

[6] T. J. Devlin, B. C. Barish, W. N. Hess, V. Perez-Mendez, and J. Solomon; Phys. Rev. Letters **4**, 242 (1960).

[7] Michael J. Longo and Burton J. Moyer, following paper, [Phys. Rev. **125**, (1962)].

II. EXPERIMENTAL METHOD

The transmission of a well-defined beam of desired momentum through liquid hydrogen was measured. Pions were produced by collision of the internal circulating proton beam of the Bevatron with a $1\frac{1}{2}$-in. platinum target. A selected beam of them was brought to the hydrogen target by a magnetic optical system, and was monitored by a series of scintillation counters. The experimental arrangement is shown in Fig. 1. Since the pions emerge through a region free of magnetic field, the selection of π^+ or π^- mesons is accomplished simply by choice of current directions in the bending magnets and optical system.

A. Beam Optics

The optical system shown in Fig. 1 consists of an 8-in.-bore focusing quadrupole doublet with two 32-in.-long sections, an 18×36-in. H-type bending magnet, and a 4-in.-bore focusing quadrupole triplet with section 8 in., 16 in., and 8 in. long. We refer to these below as Q_1, B, and Q_2, respectively.

Pions emitted from the platinum target at 36.5° from the forward direction of the circulating proton beam were collected by Q_1, the effective aperture of which subtended a solid angle of approximately 2 msr at the platinum target. Quadrupole Q_1 was operated in a manner designed to bring the beam to a focus at the final transmission counter M_3, which served as a momentum-selecting counter.

Quadrupole Q_2 acted as a field lens to optimize the flux of particles through M_3 and the hydrogen target. It increased the flux through M_3 by approximately a factor of two.

The momentum analysis of the beam was accomplished by the bending magnet B, which produced a 23.28° mean angle of bend. The beam incident on counter M_3 had a width in energy at half maximum of approximately $1\frac{1}{2}$%.

Since determination of the kinetic energy or momentum of the beam was of great importance, the current

TABLE I. Counter geometries.

Counter	Diameter (in.)	Thickness (in.)	Solid angle for counter positions (msr) I	II	III
M_1	2.00	0.25	...	...	...
M_2	4.00	0.50	...	...	...
M_3	1.50	0.25	...	...	...
S_0	8.00	0.50	...	...	...
S_1	10.60	0.50	7.13	7.13	...
S_2	11.00	0.50	7.03	6.868	7.00
S_3	12.00	0.50	4.88	5.606	6.00
S_4	12.00	0.50	3.76	4.344	5.00
S_5	12.00	0.50	2.64	3.082	4.00
S_6	12.00	0.50	1.52	1.82	3.00

in the bending magnet necessary to produce a particle of given momentum in the system was measured carefully. The curve of momentum vs magnet current was measured four times, utilizing the wire-orbit technique, while the magnet was in place. All measurements agreed to approximately 1%.

The pressure curves taken with the gas Čerenkov counter described below were consistent with the wire-orbit measurements on the magnet, the threshold pressure for counting pions occurring at the point expected from the magnet measurements.

B. Hydrogen Target

The liquid-hydrogen target is described in detail in reference 8. It was designed specifically for transmission experiments using high-energy particles. Since the density of liquid hydrogen is so low (0.071 g/cc), the target was made quite long in order to obtain a reasonable attenuation of the beam, and thus good statistical accuracy. The length of the hydrogen flask was $48\frac{7}{8}$ in. between centers of the Mylar end windows with 1 atm pressure difference. The large diameter of the flask (4 in.) prevented any particles counted by the final $1\frac{1}{2}$-in. diam scintillation counter from illuminating the target walls.

C. Counters

All the counters except the Čerenkov ones were plastic scintillation counters made of a solid solution of terphenyl in polystyrene. Sizes are listed in Table I. All the scintillators were viewed through Lucite light pipes by RCA 6810A photomultiplier tubes. High-capacitance tube bases were used throughout because of the high singles counting rates expected in tubes exposed to the main pion beam.

Counters M_1 and M_3 determined the geometry of the pion beam incident on the hydrogen target. Their sizes represent a compromise between the need to obtain a high counting rate for good statistical accuracy, and that of keeping the divergence of the beam low in order to prevent a large Coulomb-scattering effect and illumination of the target walls.

Counter M_2 did not define the geometry of the beam. Its purpose was to reduce the number of accidental counts in the monitor system.

Counter S_0 was placed close to and immediately following the hydrogen target in such a way that all particles that struck the transmission counters had to pass through it first. The large-area transmission counters, with their consequent high-background counting rates, necessitated the use of S_0. Its purpose was to provide a triple coincidence with the output of the monitor coincidence circuit and each of the transmission counters, thus reducing the accidental counting rate.

The transmission counters S_1 through S_6 subtended various solid angles from the center of the hydrogen target. Counter S_1 was kept at 7 msr throughout the experiment. Counter S_6, subtending the smallest solid angle, was moved several times. At the higher energies it subtended about 1.5 msr and, at lower energies, 3 msr. The change was made because the greater amount of Coulomb scattering at lower energies in the smaller solid angles made the data dubious. The other counters were moved also, to maintain equal intervals of solid angle from S_1 to S_6. The three sets of solid angles used are listed in Table I. The use of cross sections measured at various angles to extrapolate to perfect geometry is discussed in Sec. III-G.

D. Gas Čerenkov Counter and Pressure Curves

The gas Čerenkov counter is described in detail in reference 9. It served a twofold purpose in the experiment: (a) to continuously reject protons in the positive beams, and (b) to determine, by means of pressure curves, the number of protons, muons, and electrons contaminating the pion beams.

The effective volume of the gas counter was a cylinder 7 ft long and 4 in. in diameter, filled with sulfur hexafluoride as the radiating material. The pion beam was attenuated by about 35% because of scattering in this counter. When used in the monitor to reject protons, the counter was kept at a pressure of 230 psig, corresponding to a threshold velocity for Čerenkov radiation of 0.985 c, which was adequate for counting pions with kinetic energy above 675 Mev. Below this energy a liquid-nitrogen counter, described below, was used. Throughout the energy range of the experiment, the velocities of the protons were well below the threshold velocity of the gas counter. The efficiency of the gas counter for counting pions was about 95%, determined on negative beams by calculating the ratio of coincidences between the Čerenkov counter and M_2M_3C, to coincidences in M_2M_3 alone.

[8] Duane B. Newhart, Victor Perez-Mendez, and William H. Pope, Lawrence Radiation Laboratory Report UCRL-8857, 1959 (unpublished).

[9] John H. Atkinson and Victor Perez-Mendez, Rev. Sci. Instr. **30**, 865 (1959).

No adequate method was found for measuring the efficiency of the gas counter for counting protons. It was assumed to be zero. The possibility that delta rays produced in the counter by protons would give enough Čerenkov light to be counted was investigated. It was calculated that a number of protons (about 10% at the highest energies encountered in the experiment) produced δ rays with velocities above the Čerenkov threshold; however, the maximum energy of the δ rays thus produced was just barely above the threshold, and the amount of light collected by the phototube was insufficient to produce a signal of appreciable size.

Although the Čerenkov counter itself was probably 100% efficient in rejecting protons, the total monitoring system was only 93 to 98% efficient for proton rejection. The lowered efficiency was due to accidental coincidences in the Čerenkov counter. This is discussed in more detail in Sec. III-F.

Contamination of muons and electrons in the beam was measured by the pressure-curve method, in which the response of the Čerenkov counter was determined as a function of the pressure of the gas in the counter at constant temperature. The index of refraction of the gas is given as a function of pressure at room temperature in reference 9. One of the curves obtained is shown in Fig. 2, in which the various constituents of the beam are clearly shown. These measurements, including the function of the copper mentioned in Fig. 2 are discussed in Sec. III-E.

E. Liquid-Nitrogen Čerenkov Counter

For measurements of the π^+ cross section from 450 Mev through 675 Mev, a liquid-nitrogen Čerenkov counter was substituted for the gas counter. The index of refraction of liquid nitrogen ($n=1.2053$ at its boiling point) was adequate to separate pions from protons in this energy range.

Qualitative checks on the counter showed it to be nearly 100% efficient. Since any inefficiency would have no effect on the cross section, no attempt was made to determine it exactly.

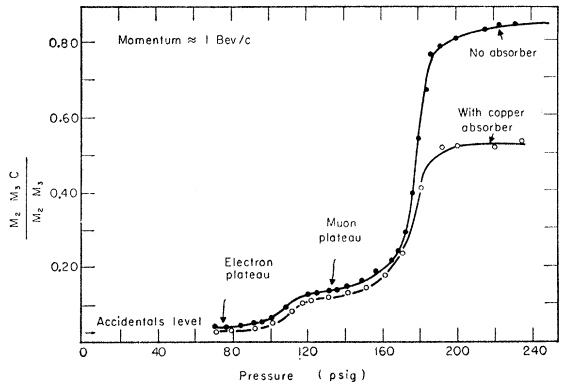

FIG. 2. Pressure curves for gas Čerenkov counter.

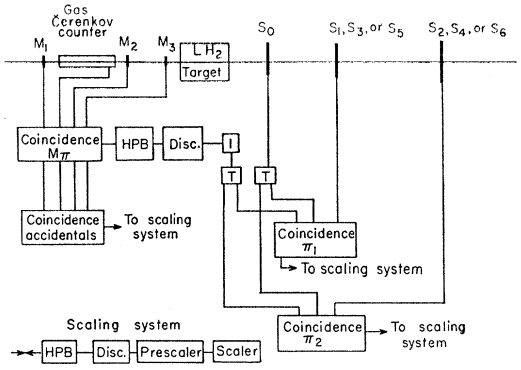

FIG. 3. Block diagram of electronics. Not all coincidences are shown. Signals from M_π and S_0 are continued through coincidence π_1 and into another coincidence with counter S_3, and subsequently with S_5 and the beam-distribution counter. Likewise, coincidence π_2 begins another chain of coincidence circuits yielding information on counters S_1 and S_6, and finally an accidentals measurement. At diagram center, I is a pulse inverter and the T's are pulse splitters.

F. Electronics

The block diagram of the electronics system for this experiment is shown in Fig. 3. The setup was exactly the same for both positive and negative beam, except that the Čerenkov counter was physically removed from the negative beam and the monitor coincidence circuit was changed accordingly.

The coincidence circuits were all of the Wenzel type.[10] The monitor and monitor-accidentals coincidence circuits were modified to provide a fourfold coincidence. All the others were of the standard threefold type. Swift-Perez-Mendez discriminator-amplifiers were used throughout the system.[11] The distributed amplifiers employed were Hewlett-Packard 460A and 460B. The prescalers were Hewlett-Packard 520A, and the scalers were of the type described in the Lawrence Radiation Laboratory Counting Handbook.[12]

III. ANALYSIS OF THE DATA

A. General

If we let $I=I_e$ be a measurement of transmitted intensity when the target is empty, and $I=I_f$ be the same measurement with a full target, then we have

$$\sigma=(1/nx)\ln(I_e/I_f),$$

where n, x, and σ refer only to the liquid hydrogen and are, respectively, the number of hydrogen nuclei per cm^3, the length in cm of the beam path in hydrogen, and the attenuation cross section in cm^2 per hydrogen nucleus.

[10] William A. Wenzel, University of California Radiation Laboratory Report UCRL-8000, 1957 (unpublished).

[11] David F. Swift and Victor Perez-Mendez, Lawrence Radiation Laboratory Report UCRL-8569, 1958 (unpublished).

[12] Lawrence Radiation Laboratory Counting Handbook, Lawrence Radiation Laboratory Report UCRL-3307 Rev., 1959 (unpublished).

In this experiment, I_e and I_f were given by the ratios of transmission coincidences to monitor coincidences (see Fig. 1),

$$I=M_1M_2M_3CS_0S_i/M_1M_2M_3C,$$

where i refers to any one of the transmission counters, S_1 to S_6.

In this way, a cross section was calculated for each of the transmission counters. The results were corrected for accidentals, muon and electron contamination, and Coulomb scattering. Then the resulting cross sections, as functions of solid angle, were extrapolated to zero solid angle. In the case of the π^+-p cross sections, a further correction was applied for contamination of the beam by protons. These corrections are described in detail below.

B. Energy Corrections

It was necessary to correct the energy determined by the bending magnet because of energy losses in air, counters, target walls, and the hydrogen itself. This was done by using range and dE/dx tables.[13] The correction amounted to about 25 Mev in the π^- beam, but about 80 Mev in the π^+ beam due to the presence of the Čerenkov counter.

Although the accuracy of the energy measurement was about $1\frac{1}{2}\%$, the energy spread, i.e., the band of energies involved in any one cross-section measurement, was about ± 20 Mev from the central energy. This was because the hydrogen target was so long. Therefore, all cross sections measured in this experiment represent an average over 40 Mev in energy. It is to be expected that this has little effect on the results in regions where the slope of cross section vs energy is relatively constant, but one must examine the effect at peaks and valleys in the cross section where the slope is rapidly changing. The effect of averaging over a band of energies was investigated in some detail in the region of the peaks in the cross section and was found to be negligible (of the order of 0.2 mb, with an uncertainty about the same).

C. Accidentals Corrections

Most types of accidental counts have only a small effect on the results of a transmission experiment. However, there is one type that changes the value of the apparent cross section by a percentage approximately equal to the percentage of accidental counts—that in which a particle scattered by the hydrogen appears to be unscattered because of an accidental count in the transmission counter. However, qualitative considerations show that this effect, for the conditions of this experiment, is corrected by the extrapolation to zero solid angle. No explicit correction was made.

[13] John H. Atkinson, Jr. and Beverly Hill Willis, University of California Radiation Laboratory Report UCRL-2426 Rev., 1957 (unpublished).

D. Coulomb Scattering Correction

Because of the length of the hydrogen target, the measurement of the total cross section was affected appreciably by Coulomb scattering at the lower momenta and smaller solid angles. Coulomb scattering in the target walls, counters, etc., was automatically corrected for by the target-empty effect, so that only the hydrogen itself was considered in the correction.

Except for the value of the mean scattering angle, the method used was essentially that of Sternheimer.[14] The mean scattering angle quoted by that author was found to yield a correction obviously too large. In several measurements taken early in the experiment, before optimum beam tuning had been attained, the Coulomb scattering effect on the counter with smallest solid angle was extremely large—of the order of 10 mb. These cases were selected for revision of the value of the mean scattering angle. The results indicated that Sternheimer's value, revised by a factor of 0.69, gives consistent sets of corrections. This factor is somewhat smaller than that indicated by Molière theory.[15]

In order to employ the Sternheimer method, the flux of particles at the transmission counter must be known as a function of position over the face of the counter. This was measured by a "beam distribution counter" consisting of a small scintillation counter and long, thin light pipe mounted on a frame horizontally and vertically movable in a plane perpendicular to the beam direction. Beam distributions were measured before and after the bank of transmission counters, and the results were interpolated to the positions of the individual counters. Distribution measurements were taken concurrently with almost every measurement of a cross section. The corrections to those few cross sections that lacked a beam-distribution measurement were inferred from corrections calculated under similar experimental conditions.

E. Muon and Electron Contamination

Contamination of the beam by muons is divided into two separate contributions: pion decays before and after the bending magnet. The contribution from decays after the magnet was determined by calculation alone, since the method is quite straightforward. Calculation of the contribution from decays before the magnet is much more difficult, but the pressure curves for gas Čerenkov counters provided a good check on the validity of the result. The agreement between measured and calculated values was excellent.

Since the bending magnet is a momentum-selecting device, all the muons produced before the magnet and deflected into the counter telescope have the same momentum as the accepted pions. This allows separa-

[14] R. M. Sternheimer, Rev. Sci. Instr. **25**, 1070 (1954).

[15] Walter H. Barkas and Arthur H. Rosenfeld, University of California Radiation Laboratory Report UCRL-8030, 1958.

tion of the two particles by the difference in their velocities with the gas Čerenkov counter. Starting at high pressure, all the pions, muons, and electrons were counted. Lowering the pressure successively eliminated pions and then muons (Fig. 2). Comparison of the relative heights of the electron, muon, and pion plateaus gave the percentage of contamination of muons and electrons from contributions before the bending magnet. Muons produced after the magnet have a wide spectrum of momenta and tend to decrease the sharpness of delineation of the components from before the magnet, but contribution of the former is calculable.

In order to check on whether the second plateau was really muons, an amount of copper corresponding to one pion nuclear mean free path was inserted in front of the third telescope scintillation counter. It was expected that essentially all the muons should get through, since Coulomb scattering losses at these energies should be negligible. The strongly interacting pions should be substantially attenuated. The measurements, shown in Fig. 2, verify this.

The pressure curves were repeated at several energies, giving a measure of the contamination as a function of energy. The final results for muon contamination, obtained from measurement and calculation, are shown in Fig. 4.

At the higher energies, contamination of the beam by electrons was very small, of the order of 1%, found by comparing the relative counting rates with various quantities of lead inserted into the path of the beam, and by examining the pressure curves in the region where only electrons could count. The counting rates on the electron plateau were just slightly higher than the background rate of accidentals, and were, for this reason, rather difficult to determine exactly.

At lower energies, the number of electrons in the beam was somewhat higher. Subtraction of the accidentals rates indicated that the contamination might be as high as 5% at the lowest energies.

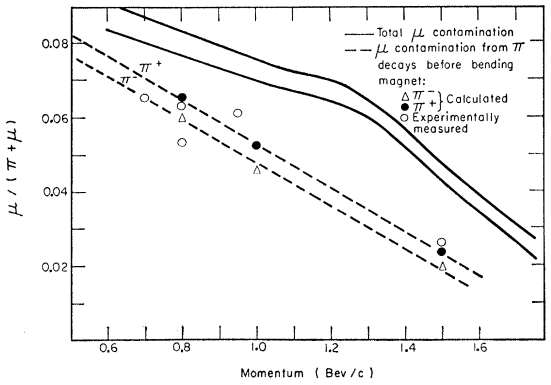

FIG. 4. Contamination of the pion beams by muons. The dashed curves represent the contribution from decays before the bending magnet, and the plotted points refer to these curves. The solid curves represent the total muon contamination from decays both before and after the magnet. The reason for the difference between the positive and negative muon contaminations is attenuation of the positive pions in the Čerenkov counter.

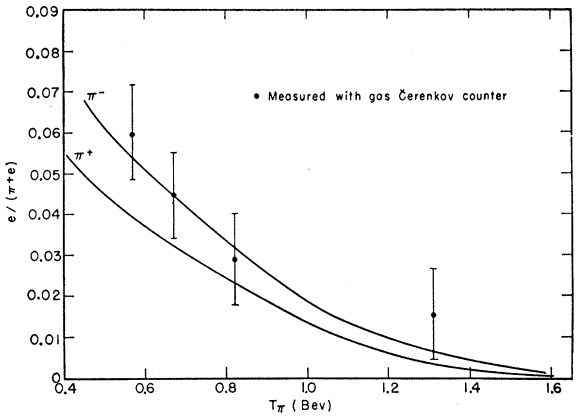

FIG. 5. Contamination of the pion beams by electrons. The curves represent the calculated values renormalized to the measured point at 650 Mev. The difference between the values for positive and negative beams is a combination of the branching ratios for producing positive and negative pions in the platinum target, and attenuation of the positive beam by the Čerenkov counter.

An attempt was made to calculate the amount of electron contamination from the spectrum of neutral pions produced in the target, the amount of platinum in the path of the gammas arising from decay of the pions, and the energy spectrum of the pair-produced electrons. Some very crude approximations were necessary in order to simplify the calculation. The results yielded contaminations roughly 50% higher than those measured by the Čerenkov counter. Although the approximations used in the calculation were probably crude enough to give invalid results for the absolute value of the contamination, it is felt that the energy dependence is substantially correct. Therefore, the calculations were renormalized to the best of the Čerenkov counter measurements, and these values were used to correct the data. The other Čerenkov counter measurements were consistent with the renormalized calculations. The electron contamination as a function of energy is shown in Fig. 5.

F. Proton Contamination

The positively charged beam of particles was composed of approximately 75% protons and 25% pions. These percentages were determined by use of the gas Čerenkov counter, set at a threshold above that for counting protons and below that for counting pions. The counter was put into coincidence with the scintillation counters that monitored the beam incident on the hydrogen target. Ideally, this system would count only the pions. However, because of a type of accidental coincidence previously mentioned in Sec. II-D, its efficiency for rejecting protons varied between 93 and 98%, depending on the running conditions. This species of accidental counts was monitored continu-

ously throughout the experiment. The *counted* beam varied between 5 and 15% protons, depending on experimental conditions, with the rest pions and muons. These rates are consistent with an instantaneous rate of 10^6 background counts per second in the Čerenkov counter. Considering its position, lack of shielding, and the radio-frequency structure of the beam, this is quite a reasonable figure to expect.

Several checks verified that there really were protons in the counted beam, the simplest of these being that on negative beam the accidentals rates of the type considered above were much smaller and quantitatively consistent with the counting rates involved.

The known proton-proton cross section and the measured percentage of protons in the counted beam were used to correct the data in an obvious manner. The correction to the π^+-p cross section was typically of the order of 1 mb or less, yielding a value less than the uncorrected value.

Some uncertainty remains in relating the measured rate of accidentals to the true rate, because of the rf structure of the beam intensity. One extreme estimate of this effect, based upon the worst possible beam-structure assumption, indicated a maximum change of about 15% in the correction, i.e., less than 0.15 mb change in the correction cross section. The true change necessary to compensate for the rf structure is certainly less than this. Since this correction is so small, well within the statistics on the points, no attempt has yet been made to evaluate it exactly.

G. Extrapolation to Zero Solid Angle

Under ideal conditions, a transmission counter of finite size measures an apparent total cross section, equal to the true total cross section diminished by an amount equal to the integral from zero to the half-angle subtended by the counter of the angular distribution of all charged particles resulting from interactions and scattering events. We may write this as

$$\sigma_M=\sigma_T-2\pi\int_0^{\theta_1}\frac{d\sigma_{\rm ch}}{d\Omega}\sin\theta d\theta,$$

where σ_M is the measured value of the cross section, σ_T is the true value, and $d\sigma_{\rm ch}/d\Omega$ is the value of the angular distribution for all charged particles. This angular distribution includes both the elastic angular distribution and that for emission of charged secondaries in the forward direction from inelastic events. The limit of integration θ_1 is the half-angle subtended by the transmission counter.

If several transmission counters subtending different angles are used, the graph of apparent cross section vs solid angle should lie on a line with a slope equal to the negative of the total charged differential cross section at 0° in the laboratory system, and which passes through the true value of the total cross section at zero solid angle. This is true only if the angles involved are small enough so that the differential cross section can be considered constant and equal to its value in the forward direction.

Under more realistic conditions, however, both the slope and the intercept of the line used in the extrapolation may be changed by various extraneous effects. Some of these are accidental counts, Coulomb scattering, nuclear scattering in counters, muon contamination, etc. Of these, only the Coulomb scattering changes the intercept—i.e., the true value of the total cross section—and this correction was applied explicitly. For all the others, including the prevalent type of accidental counts, in those cases in which there was an appreciable effect at finite solid angles, the correction was found to extrapolate to zero with solid angle.

Thus we have the result that the slopes of the lines used in the extrapolation are not those inferred from the expected angular distributions; in fact, they are considerably larger. Because of the relatively small number of points available for the determination of the slope (five or six), the errors involved are fairly large. However, they showed a fairly consistent tendency to remain in the range from −0.4 through −0.1 mb/msr. Because of the poor statistics involved, the slope finally employed at any given energy was the average of slopes calculated for that energy and nearby energies.

Because of the small angles involved, and the small value of the slope, any uncertainty in the slope has a relatively small effect on the total cross section. The

TABLE II. Summary of total cross-section results.

π^+-p			π^--p		
T_π (Mev)	σ_T (mb)	$\Delta\sigma$ (mb)	T_π (Mev)	σ_T (mb)	$\Delta\sigma$ (mb)
457	29.44	1.63	452	33.03	0.69
506	24.14	2.11	503	36.01	0.61
529	22.87	1.80	554	41.86	0.81
651	17.95	1.34	598	46.20	0.84
749	21.58	0.65	652	41.67	0.78
805	24.98	0.74	705	40.23	1.05
861	27.10	0.50	727	40.66	0.58
890	25.79	0.39	755	42.09	0.88
906	27.04	0.80	800	44.71	0.76
952	26.98	0.66	852	52.74	0.63
998	28.90	0.58	873	55.97	0.71
1042	29.69	0.44	896	57.82	0.84
1100	31.80	0.44	920	56.95	0.86
1146	35.70	0.58	962	51.75	0.85
1183	36.76	0.41	993	46.66	0.64
1240	39.53	0.72	1022	42.37	0.62
1336	41.56	0.58	1045	41.17	0.59
1440	39.53	0.50	1100	37.18	0.61
1510	39.27	0.74	1150	36.55	0.71
			1195	35.84	1.22
			1240	35.22	0.60
			1300	35.72	0.93
			1347	35.41	0.46
			1416	34.51	0.54
			1456	34.62	0.58
			1520	33.81	0.73
			1548	33.90	0.46
			1584	33.40	0.46
			1650	27.08	0.96

uncertainty in the slope has been included as part of the errors on the calculated values of the cross sections.

Figure 6 gives examples of the extrapolation. A least-squares fit was used to calculate the slope and intercept of the lines. The slopes for all energies were then examined for consistency. In the case of the negative pions, they averaged about -0.22 mb/msr, with no discernible dependence on energy. For positive pions, the slopes increased with energy from about -0.2 at 900 Mev to -0.4 at 1600 Mev. The most likely explanation of this behavior is the production of charged secondary particles by protons contaminating the beam. Below 900 Mev the slopes get larger in absolute value, probably because of inaccuracies in the relatively large Coulomb correction applied, and the Coulomb scattering of the accidentally counted protons. The energy dependence of the slopes was continued below 900 Mev as determined from higher energies, and the lines used in the extrapolation were forced to fit the slopes thus determined. This fact, and the uncertainties in the Coulomb corrections in this energy range, are reflected in the relatively large errors on the points in this region.

IV. RESULTS

The measured values of the total cross sections for π^+-p and π^--p reactions are listed in Table II, and graphed as a function of lab pion kinetic energy in Figs. 7 and 8.

The uncertainties listed are a combination of the counting statistics, and uncertainties in the corrections applied. In several cases, the values of the cross section

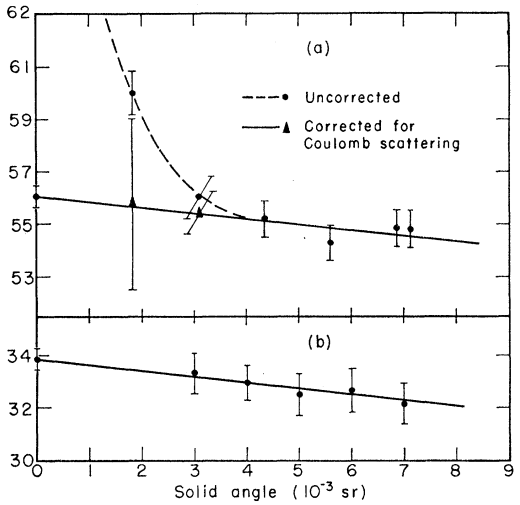

FIG. 6. Plots of apparent total cross section as a function of the solid angle subtended by the transmission counter. Curve *a*, taken at 895 Mev and before optimum beam tuning, shows an appreciable Coulomb-scattering effect in the smaller solid angles. Curve *b*, taken at 1548 Mev with good beam tuning, has a negligible Coulomb effect. The line represents a two-parameter least-squares fit to the corrected points. The correction for muon contamination, dependent on solid angle, is included in the values plotted. Electron contamination and other corrections are not included, since they are not dependent on solid angle.

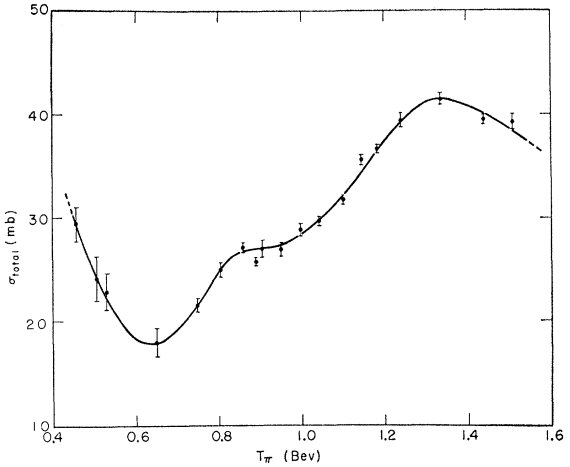

FIG. 7. Total cross section for π^+-p as a function of laboratory pion kinetic energy.

represent two or three measurements all within the 40-Mev energy band under study, combined to give a weighted average of the cross section. In two cases, deviation of the individual points from the average was greater than one standard deviation. In these, the rms deviation was substituted for the calculated uncertainty.

The group working at Saclay, France, has performed a similar experiment[5] over most of the energy range covered in this one. Their results for the negative-pion scattering are in excellent quantitative agreement with the results quoted here. Although the qualitative features of their results for positive pions are the same, there is a systematic discrepancy of about 2 to 3 mb between the two experiments, with our experiment exhibiting the higher results. This discrepancy has not been explained, but might be ascribed to differences in the geometric correction or beam contamination. Careful reexamination of all the data and corrections involved in this experiment reveals no justification for revising the results presented.

The slight difference between the data presented here and those presented in a previous report of this experiment[6] is due to a more complete analysis of the corrections made to the measurements.

Longo *et al.* have extended the π^+-p data to higher energies in a separate experiment designed to provide desirable π^+ beam intensities up to 4 Bev.[7]

V. DISCUSSION

In the following paragraphs we calculate the cross section for the pure eigenstate of isotopic spin, $T=\frac{1}{2}$, discuss possible assignments of the quantum numbers for resonant states, and quote the results of a calculation of the real part of the forward scattering amplitude on the basis of dispersion relations. We also compare the scattering measurements with pion photoproduction measurements in regard to energy dependence.

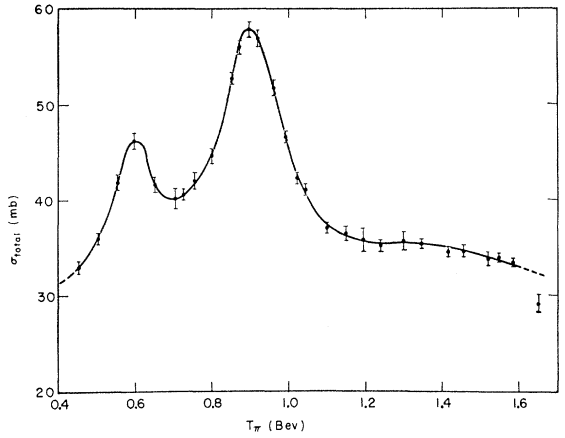

FIG. 8. Total cross section for $\pi^- - p$ as a function of the laboratory pion kinetic energy.

A. Cross Section for Pure $T=\frac{1}{2}$ State

Under the assumption of charge independence, all the strong interactions between pions and nucleons can be described in terms of two eigenstates of isotopic spin. The pion has an isotopic spin of 1, and the nucleon, $\frac{1}{2}$. The total isotopic spin of the system consisting of one pion and one nucleon can thus be either $\frac{3}{2}$ or $\frac{1}{2}$. Charge independence states that, in isotopic spin space, the behavior of the system depends only on the value of the total isotopic spin and is independent of its projection on the z axis. Thus, the isotopic spin part of the wave function of any of the six charge states in the pion-nucleon system may be written as a linear combination of the two eigenstates of isotopic spin. If we develop the expressions for the total cross section we find, for the two cases under consideration in this experiment,

$$\sigma(\pi^+ - p) = \sigma(\tfrac{3}{2}),$$

and

$$\sigma(\pi^- - p) = \tfrac{2}{3}\sigma(\tfrac{1}{2}) + \tfrac{1}{3}\sigma(\tfrac{3}{2}).$$

Solving these two equations for the pure $T=\frac{1}{2}$ state, we find

$$\sigma(\tfrac{1}{2}) = \tfrac{3}{2}\sigma(\pi^- - p) - \tfrac{1}{2}\sigma(\pi^+ - p).$$

The results of a calculation of this cross section in the energy range under consideration are presented in Fig. 9.

Qualitatively, the general features of the $T=\frac{1}{2}$ cross section are the same as those of the $\pi^- - p$ cross section. The main difference is in the heights of the peaks, 60.2 mb at 600 Mev, and 73.2 mb at 900 Mev, and in the behavior of the flat portion of the curve above 1200 Mev. The $T=\frac{1}{2}$ cross section drops rapidly to a value below 32 mb, and is consistent with an asymptotic approach to the high-energy (4-Bev) value of about 30 mb.[16] Thus, the plateau observed in the $\pi^- - p$ cross section between 1.1 and 1.4 Bev can be ascribed to a contribution from the broad maximum in the pure $T=\frac{3}{2}$ state.

B. Resonant States

If the expression for the total cross section is developed in terms of a partial-wave expansion of the scattering amplitudes for pion-nucleon scattering, we find that the maximum possible contribution from a given partial wave to the total cross section can be written

$$\sigma(l,J) = \pi\lambda\!\!\!^{-2}(2J+1)(1+b),$$

where $\sigma(l,J)$ is the contribution to the total cross section from that partial wave having orbital angular momentum l and total angular momentum J; $\lambda\!\!\!^{-}$ is the deBroglie wavelength of the pion in the center-of-mass system, and b is an inelastic-scattering parameter which takes on values between 0 for pure diffraction scattering, and 1 for purely elastic scattering. We assume that we are dealing with the cross section for a pure isotopic spin state, and that the partial wave under consideration is in resonance, i.e., the phase shift $\delta_{l,J}$ is 90°.

Let us examine the peaks in the $T=\frac{1}{2}$ isotopic spin state at 600 Mev and 900 Mev in the light of the above equation. Some qualitative observations are necessary to justify the procedure to be adopted. First, the widths (of the order of 150 Mev) and general shapes of these peaks are not unlike that of the 3–3 resonance in the $T=\frac{3}{2}$ cross section at 200 Mev. Since the behavior of the pion-nucleon cross section in the neighborhood of 200 Mev is quite adequately explained by a resonance in the state where $l=1$, $J=\frac{3}{2}$, and $T=\frac{3}{2}$, we are somewhat justified in assuming that the peaks at 600 Mev and 900 Mev are also due to resonant states. Secondly, there is an appreciable contribution to the cross section from partial waves other than the one in

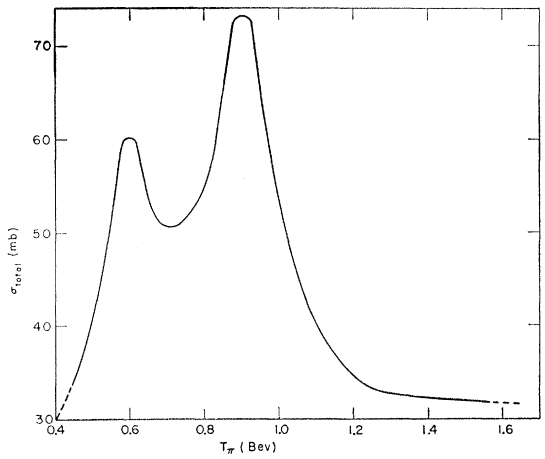

FIG. 9. Total cross section for pure isotopic spin state $T=\frac{1}{2}$ as a function of the laboratory pion kinetic energy.

[16] N. F. Wikner, University of California Radiation Laboratory Report UCRL-3639, 1957 (unpublished).

resonance. Goodwin indicates that, above 427 Mev, all partial waves up to F waves have a non-negligible contribution to the angular distributions.[17] Thus, in analyzing the total cross section, we must subtract a "nonresonant background" contribution from states other than the one in resonance.

If we assume that the nonresonant part of the cross section is about 30 mb—i.e., approximately equal to the asymptotic value of the total cross section at high energies—we can solve the above equation for b, trying several different values of the total angular momentum J. The results are shown in Table III.

At 600 Mev, the results are fairly clear, subject, of course, to the validity of the assumption about the nonresonant contribution. If, in fact, this is a resonant state, it probably has $J=\frac{3}{2}$, with a fairly high amount of inelastic scattering. This conclusion is substantiated to some extent by data from a number of experiments collected by Falk-Vairant and Valladas and presented at the 1960 Rochester Conference.[18] Measurements of the total elastic cross section (and by subtraction, the total inelastic cross section) indicate the presence of a peak in both the elastic and inelastic cross sections at this energy. Qualitatively, this is the behavior to be expected from the value of b quoted in Table III for $J=\frac{3}{2}$. The assignment of $J=\frac{3}{2}$ is also consistent with an analysis of the angular distribution for pion photoproduction,[4] which indicates that the proper assignment of quantum number for this resonance is $l=2$, and $J=\frac{3}{2}$.

At 900 Mev the results are somewhat ambiguous. With an assignment of 30 mb for the nonresonant contribution, three values of J fall in the acceptable range.

TABLE III. Values of the inelastic coefficient for various assumptions about total angular momentum and nonresonant contribution.

T_π (Mev)	σ(total) (mb)	σ(nonresonant) (mb)	σ(resonant) (mb)	J	$\pi\lambda^2(2J+1)$	b
600	60.2	30	30.2	1/2	12.00	>1
				3/2	24.1	0.251
				5/2	36.2	<0
900	73.2	30	43.2	3/2	14.9	>1
				5/2	22.4	0.93
				7/2	29.8	0.45
				9/2	37.3	0.16
				11/2	44.8	<0
900	73.2	40	33.2	3/2	14.9	>1
				5/2	22.4	0.48
				7/2	29.8	0.11
				9/2	37.3	<0

[17] Lester K. Goodwin, Ph.D. Thesis, Lawrence Radiation Laboratory Report UCRL-9119, 1960 (unpublished); L. K. Goodwin, R. W. Kenney, and V. Perez-Mendez, Phys. Rev. Letters **3**, 522 (1959), also, Phys. Rev. **122**, 655 (1961).

[18] P. Falk-Vairant and G. Valladas in *Proceedings of the 1960 Annual International Conference on High-Energy Physics at Rochester* (University of Rochester; Interscience Publishers, Inc., New York, 1960), p. 38.

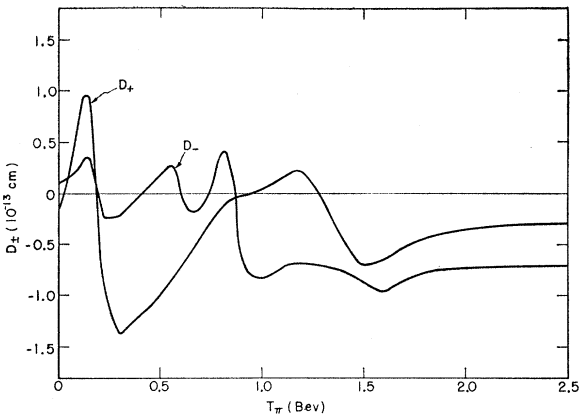

FIG. 10. Real part of the forward scattering amplitude for positive D_+ and negative D_- pions on protons, as a function of the laboratory pion kinetic energy.

Although not impossible, it seems unlikely that J is $\frac{9}{2}$. The indications of a peak in the inelastic cross section near 900 Mev[18] seem to rule out $J=\frac{5}{2}$ because of the value of b, which is very close to 1.0. However, analysis of photoproduction results,[4] although not conclusive, tends to favor the assignment of $J=\frac{5}{2}$. These contradictory conclusions may be resolved if we assume a different value for the nonresonant contribution.

If this contribution in the vicinity of 900 Mev has a value of about 40 mb, for some reason not clearly understood but possibly inferable from the angular distributions in Wood's data,[19] then the value of b for $J=\frac{5}{2}$ is more consistent with a substantial amount of inelastic scattering.

A recent experiment at Berkeley measured the elastic angular distribution for π^--p scattering.[19] Although not yet completely analyzed, it is consistent with the suppositions of $J=\frac{3}{2}$ and $J=\frac{5}{2}$ for the two states, respectively, subject to the validity of the assumption that they are in resonance.

Some speculation has been made about the possibility that there is a resonance in the π^+-p interaction near 800 Mev.[20] The behavior of the total cross section in this energy range gives some support to this view. However, in view of the fact that the nonresonant part of the cross section is not well known, an analysis similar to that presented above is inappropriate. The confirmed existence of a resonant state must await angular distribution and polarization measurements.

C. Application of Dispersion Relations

The real part of the forward scattering amplitude for pion-proton scattering may be determined from the

[19] C. D. Wood, T. J. Delvin, J. A. Helland, M. J. Longo, B. J. Moyer, and V. Perez-Mendez, Bull. Am. Phys. Soc. **5**, 509 (1960); Also, Phys. Rev. Letters **6**, 481 (1961).

[20] Peter Carruthers, Phys. Rev. Letters **4**, 303 (1960).

imaginary part by the dispersion relations.[21] The calculation involves integrals of the imaginary part over all energies. Since the imaginary part of the forward scattering amplitude is related to the total cross section by the optical theorem, the real part may be determined from the behavior of the total cross section. Explicitly, we have

$$D_{\pm}(k)=\tfrac{1}{2}(1\pm\omega/\mu)D_{+}(0)+\tfrac{1}{2}(1\mp\omega/\mu)D_{-}(0)$$
$$+\frac{k^2}{4\pi^2}P\int_{\mu}^{\infty}\frac{d\omega'}{k'}\frac{\sigma_{\pm}(\omega')}{\omega'-\omega}$$
$$+\frac{k^2}{4\pi^2}\int_{\mu}^{\infty}\frac{d\omega'}{k'}\frac{\sigma_{\mp}(\omega')}{\omega'+\omega}\pm\frac{2f^2}{\mu^2}\frac{k^2}{\omega\pm\mu^2/2M},$$

where $D_{\pm}(k)$ is the real part of the pion-proton forward scattering amplitude at the pion laboratory-system wave number k; ω is the total energy of the pion in the laboratory system; μ is the pion mass; $\sigma_{\pm}(\omega')$ is the total pion-proton cross section at energy ω'; and M is the nucleon mass. The units of k, ω, μ, and M are cm^{-1}; P means that the principal value of the integral is taken. The coupling constant has the value $f^2=0.08$; the starting values for the amplitudes are $D_{+}(0)=-0.148\times10^{-13}$ cm and $D_{-}(0)=+0.106\times10^{-13}$ cm.

Cronin has used the previously reported results of this experiment[6] and others[3,5,7,16] to perform this calculation. His results are contained in reference 22, and are shown in Fig. 10.

[21] M. L. Goldberger, Phys. Rev. **99**, 979 (1955); R. Karplus and M. A. Ruderman, *ibid.* **98**, 771 (1955); M. L. Goldberger, H. Miyazawa and R. Oehme, *ibid.* **99**, 986 (1955); H. L. Anderson, W. C. Davidon, and U. E. Kruse, *ibid.* **100**, 339 (1955).

[22] J. W. Cronin, Phys. Rev. **118**, 824 (1960).

D. Comparison Between Scattering and Photoproduction

We wish to compare the results of pion scattering with the photoproduction reactions

$$\gamma+p\rightarrow\pi^0+p, \quad (1)$$

and

$$\gamma+p\rightarrow\pi^+ +n. \quad (2)$$

At low energies, it is expected that the influence of the strong final-state interaction in photoproduction will dominate the reaction and show a direct correspondence with the matching situations in pion scattering. As inelastic channels become more important at higher energies, this correspondence will be somewhat less evident; however, comparisons are still worth while.

A number of experiments dealing with reaction (1) indicate the presence of a maximum in the cross section in the vicinity of 750-Mev energy (lab) of the gamma ray.[23] Other experiments[24] dealing with reaction (2) show a maximum at about 700 Mev. If we assume that the maximum in the photoproduction cross section occurs at an energy where the total energy in the c.m. system is the same as that in the pion-proton scattering situation at 600 Mev, we would expect a maximum in photoproduction at 750 Mev. Therefore, good agreement obtains between the scattering results and measurements of reaction (1). The 50-Mev difference between the scattering results and reaction (2) may be explained by a component of the photoproduction matrix which operates for charged-meson photoproduction alone.[4] No estimate of the magnitude of the effect of this term is available.

[23] J. W. DeWire, H. E. Jackson, and R. Littauer, Phys. Rev. **110**, 1208 (1958); P. C. Stein and K. C. Rogers, *ibid.* **110**, 1209 (1958); J. I. Vette, *ibid.* **111**, 622 (1958); K. Berkelman and J. A. Waggoner, *ibid.* **117**, 1364 (1960).

[24] M. Heinberg, W. M. McClelland, F. Turkot, W. M. Woodward, R. R. Wilson, and D. M. Zipoy, Phys. Rev. **110**, 1211 (1958); F. P. Dixon and R. L. Walker, Phys. Rev. Letters **1**, 142 (1958); L. Hand and C. Schaerf, *ibid.* **6**, 229 (1961).